Self-Assembly of Tetraphenylethylene-Based Amphiphiles in Aqueous Methanol Solution into Two-Dimensional Chiral Sheets for Enantioselective Sorption

Yanqiu Wang[a] and Myongsoo Lee*[b]

Most synthetic building blocks self-assemble into one- or three-dimensional architectures. However, fewer examples have been reported on the aggregation of amphiphiles to form optically-active two-dimensional (2D) structures. Herein, we report the self-assembly of tetraphenylethylene (TPE)-containing hydrophilic dendrons into 2D sheet structures in aqueous methanol solution. TEM and AFM investigations showed that the self-assembly of disubstituted TPE generates helical nanofibers as an intermediate structure which, in turn, laterally associate into a chiral sheet structure with a thickness of 4.6 nm, whereas tetrasubstituted TPE self-assembles into a nonchiral sheet structure with a thickness of 3.8 nm. In great contrast to the nonchiral sheets, the chiral sheets are able to preferentially absorb the D-enantiomer in a racemic phenylalanine derivative solution accompanied by fluorescence enhancement, thus indicating that the single-layered chiral sheets act as an enantioselective membrane that can be used for fluorescence sensing.

Fluorescent organic molecules have received considerable attention due to the interesting photophysical properties accompanied by their intrinsic softness and lightness.[1] In addition to the fluorescence emission properties exhibited in the molecular level, aggregation-induced emission (AIE) molecules are the attractive target due to switchable characteristics in response to aggregation.[2–9] The aggregation of AIE molecules plays a critical role in exhibiting novel optical properties caused by planarization during a self-assembly process which is mostly driven by aromatic interactions.[10] Tetraphenylethylenes (TPE) as an AIE-active molecule has been introduced to construct 2D networks[11] because of its potential applications such as TPE-based supramolecular-organic frameworks and metal-organic networks,[12,13] heavy metal sensing,[14] and halogen bonded assembly.[15] A number of different functional groups have been introduced to a TPE segment to exhibit unique physical properties such as sensing and imaging materials.[16] For example, Sun and Tang reported fluorescent one dimensional (1D) micro/nanostructures with controlled morphologies through self-assembly of TPE-modified systems. The nanostructures include fibers, wires, rods, and ribbons.[17] Zheng and coworkers reported AIE-active TPE-based macrocycles that are able to self-assemble into nanofibers, microtubules and hollow microspheres depending on water content in THF-water mixtures.[18] Although a great deal of effort has been devoted to creating AIE-based supramolecular structures, most of the structures are far from the internal cavities with chiral environments required to recognize selectively one enantiomer over the other.[19] Combination of self-assembled supramolecular structures and chiral properties in AIE-based materials would allow chiral recognition with sensing properties in a racemic mixture solution.

Supramolecular chirality can be induced by chiral transfer from chiral moieties into self-assembling nanostructures.[20] We envisioned that grafting chiral dendrimers on the side faces of AIE segment would generate 2D chiral supramolecular structures with enantiomer sensing characteristics. Here, we report fluorescent supramolecular 2D architectures using aromatic amphiphiles based on an AIE segment. We designed and synthesized tetraphenylethylenes (TPE) based amphiphilic molecules by grafting hydrophilic oligoether dendritic side groups. The tetra-substituted molecule (**1**) generates nonchiral 2D nanosheet structures, while the di-substituted molecule (**2**) generates chiral 2D nanosheet structures (Figure 1). Notably,

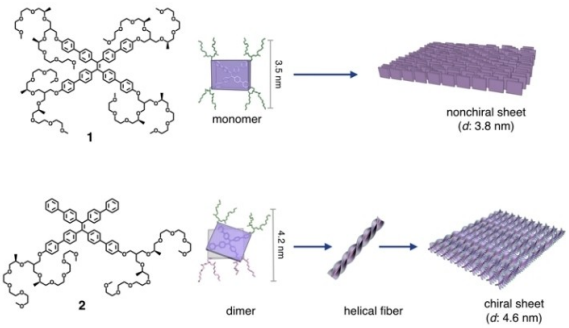

Figure 1. Molecular structures of tetra-substituted molecule (**1**) and di-substituted molecule (**2**), with schematic representations of their self-assembly.

[a] *Dr. Y. Wang*
College of Material Science and Engineering
Changchun University of Science and Technology
Changchun, 130022 (P. R. China)
[b] *Prof. M. Lee*
Department of Chemistry
Fudan University
Shanghai 200438 (P. R. China)
E-mail: mslee@fudan.edu.cn

Supporting information for this article is available on the WWW under https://doi.org/10.1002/cplu.202000130

This article is part of a Special Collection on "Supramolecular Chemistry: Young Talents and their Mentors". More articles can be found under https://onlinelibrary.wiley.com/doi/toc/10.1002/(ISSN)2192-6506.SupramolecularChemistry.

the chiral sheet structures formed from **2** are able to absorb preferentially one enantiomer over the other from racemic amino acid solution with enhanced emission properties. Thus, the molecular design combining AIE effect and chiral recognition capability offers a highly efficient strategy in constructing novel functional nanomaterials with enantiomer recognition with a sensing effect. TPE-based amphiphilic molecules were synthesized by Suzuki coupling reaction and a McMurry reaction described in the Supporting Information. The resulting molecules were characterized by ^{1}H- and ^{13}C NMR spectroscopies and MALDI-TOF mass spectroscopy were shown to be in full agreement with the structures presented.

To investigate the aggregation behavior of **1** and **2**, we have performed dynamic light scattering (DLS) experiments and fluorescence emission (FL) experiments (Figures S5, 6) by adding salt water (including 50 mM KF) into MeOH solution (0.01 wt%). The DLS data of **1** and **2** in MeOH showed to be a diameter of ~4 nm for both of the molecules which are similar with the size of the single molecules (Figure S11 in the Supporting Information), and fluorescence shows very weak emission, indicating both **1** and **2** exist as molecularly dissolved states in pure MeOH, considering that TPE-based molecules are non-emissive in the dissolved state but highly enhanced emission could be seen in both the aggregated form and the solid-state.[21] With increasing the water content up to 40% including 50 mM KF salt, both diameter and fluorescence intensity increase remarkably, indicating that addition of water into the methanol solution induces the molecular assembly. When the water fraction is further increased up to 100% (50 mM KF), the diameter of aggregates increase up to several hundreds of nanometers for both **1** and **2**, and the fluorescence is strengthened at the concentration of 0.01 wt% in water solution (50 mM KF), which indicates the formation of stable self-assembled structures. Moreover, the fluorescence of **2** shows strong blue shift with increasing the salt water fraction, which also confirm the increased π-π-stacking of aromatic cores.[22] At the same time, the absorption spectra show red shifted maximum in water solution including 50 mM KF salt compared with that in $CHCl_3$ solution (Figure S8), which further confirms aggregation behavior.

The aggregation behavior of **1** and **2** at the concentration of 0.01 wt% in aqueous salt solution has been investigated using transmission electron microscopy (TEM) and cryogenic TEM (Cryo-TEM). When the samples were cast from the aqueous solution and then negatively stained with uranyl acetate, the images of both of the molecules showed 2D flat sheet structures which was further confirmed by TEM (Figures 2a, S9). This result provides clear evidence that the aggregates exist as well-defined 2D nanostructures in bulk solution. Atomic force microscopy (AFM) experiments were performed to obtain further structural information of the nanosheet structures of **1** and **2** (Figures 2b, S10). The image of **1** revealed 2D sheet structures with a thickness of 3.8 nm, which is in reasonable agreement with the molecular dimension of **1** (Figure S11a), suggesting that the sheet structures of **1** are based on monolayer packing. The image of **2** revealed 2D sheet structures with a thickness of 4.6 nm. Considering the molecular dimension of **2** (2.4 nm from CPK) (Figure S11b), the observed thickness implies that the sheet structures consist of interdigitated bimolecular packing. Interestingly, when circular dichroism (CD) spectroscopy experiments were performed to the sheet structures, the sheet solution of **2** revealed a strong Cotton effect, in sharp contrast to that of **1** which is CD silent (Figure 2c). To gain insight into the packing arrangements of the aromatic segments within the 2D aromatic domains, we performed UV and fluorescence measurements on the sheet solutions of both **1** and **2** (Figure 2d). The absorption spectrum of **2** shows a transition with a maximum of 300 nm that is red-shifted relative to that observed in **1**. The fluorescence spectrum of **2** shows decreased emission intensity compared with **1**. Both the red-shifted absorption and the fluorescence

Yanqiu Wang received her BS degree from Jilin Normal University in 2012, and PhD degree in chemistry from Jilin University in 2017. After completion of her PhD degree, she joined at College of Material Science and Engineering at Changchun University of Science and Technology, Changchun, China as an Assistant Professor. Her research interests are supramolecular assembly and functionalized supramolecular structures, with a current focus on the development of supramolecular separation materials.

Myongsoo Lee received his BS degree at Chungnam National University, Korea and obtained his PhD degree from the Case Western Reserve University (1992) for studies on liquid crystal polymerization with Prof. V. Percec. After postdoctoral research work with Prof. S. I. Stupp at University of Illinois at Urbana (1993), he was made professor at Yonsei University, Seoul (1994), Seoul National University (2009), Jilin University (2013), and then moved to Fudan University in 2019, where he continues to work in self-assembling systems and supramolecular materials.

Yanqiu Wang joined the research group of Professor Lee as a PhD student to develop switchable supramolecular nanostructures such as inflating tubules and rolling 2D sheets. After finishing her PhD, she is carrying out independent research work in the field of supramolecular chemistry to create 2D nanomaterials for highly-efficient separations.

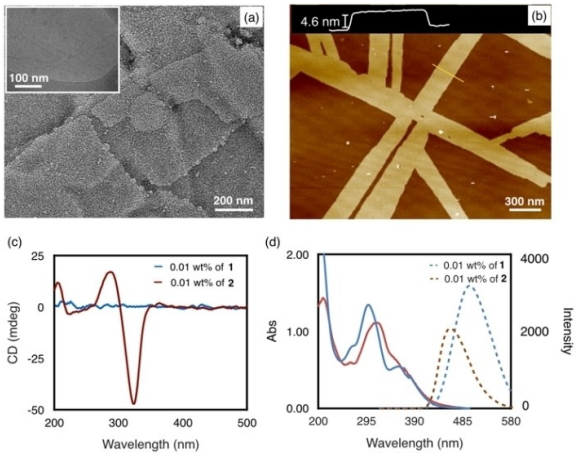

Figure 2. (a) TEM images and (b) AFM image of **2** in aqueous solution (including 50 mM KF) at 0.01 wt%, Inset: cryo-TEM of **2** in aqueous solution (including 50 mM KF) at 0.01 wt%; (c) CD experiments and (d) UV and fluorescence experiments of **1** and **2** in aqueous solution (including 50 mM KF) at 0.01 wt%.

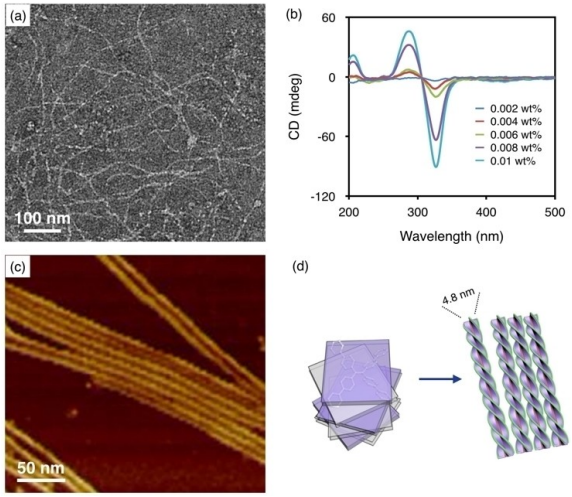

Figure 3. (a) TEM image of **2** in aqueous solution (including 50 mM KF) at 0.002 wt%; (b) concentration dependent CD spectrum of **2** in water solution (including 50 mM KF); (c) AFM image of **2** in aqueous solution (including 50 mM KF) at 0.002 wt%; (d) schematic representation of the dimers stack on top of each other to form helical fibers.

quenching are indicative of closer packing of chromophores in the sheet structure of **2**.[23]

To gain insight into the formation of the 2D sheet structures of **1** and **2**, we performed TEM experiments with a highly diluted condition (0.002 wt%). TEM image revealed that the solution of **1** showed small sheet-like aggregates at lower concentrations (Figure S12a). With increasing concentration, the small sheet fragments increase gradually in lateral dimensions to form large sheet structures (Figure S12b, 9). As reflected in the AFM image (Figure S10), the thickness of sheet structures of **1** is in agreement with the thickness of single molecule packing. Based on these observations, it can be considered that the 2D sheet structures of **1** are formed by 2D array of the aromatic segments with up and down surfaces covered by hydrophilic dendritic segments (Figure 1). We believe that the grafted 4 bulky dendritic chains lead to loosely face stacks of the TPE segments with random orientation to form 2-D sheet structures.

In great contrast, the solution of **2** showed uniform nanofiber structures with a diameter of ~4.6 nm together with a Cotton effect in the spectral range of the aromatic segments (Figure 3a, b). To investigate the CD-active fiber assembly, we performed atomic force microscopy (AFM) experiments with a highly-diluted solution (0.002 wt%) of **2** (Figure 3c). The image revealed fiber-like aggregates with an average diameter of 4.8 nm, well matched with that obtained from TEM. The fiber-like aggregates revealed a left-handed helical structure, which demonstrates that the sheet structures of **2** are originated from the lateral assembly of helical nanofibers. The dimension of 4.8 nm in diameter corresponds approximately to the lengths of bimolecular packing of **2**, suggesting that the aromatic segments are stacked on top of each other with mutual rotation in the preferred direction to form thin nanofibers with one-handed helical array, as reflected in the Cotton effect (Figure 3b, d).[24] With increasing the concentration, the elementary nanofibers further assemble through side-by-side interactions to reduce the contact between the aromatic cores of the fibers and water molecules to generate 2D sheet structures (Figures 1 and 3d).[25]

Considering that the 2D sheets of **2** consist of parallel arrangements of helical fibers, the void spaces formed between the helical fiber arrangements would be chiral with hydrophobic aromatic walls.[26] Therefore, the void spaces would readily absorb hydrophobic aromatic guest through aromatic interactions. Accordingly, we envisioned that the 2D chiral sheet functions as an enantioselective membrane as the one enantiomer over the other one preferentially bind to chiral void spaces of the chiral sheets. To explore the capability of the chiral sheets for preferential one enantiomer capture in racemic solution, hydrophobically protected phenylalanine was selected (Figure 4a). After the addition of racemic phenylalanine to the chiral sheet solution of **2** (in a mole ratio **2**/phenylalanine of 4:1) at room temperature, high-performance liquid chromatography (HPLC) and UV measurements were performed after separating out of the free racemate in the solution using a Sephadex column (Figure 4b, S13, 14). Notably, the chiral sheet structures are able to absorb preferentially one enantiomer from racemic amino acid solution with enhanced emission. HPLC with a chiral column revealed that the absorption of D-enantiomer is faster than the L-enantiomer, and showed enantiopure capture at the initial stage of absorption (up to 6 h) (Figure 4b). The preferential absorption of one enantiomer over the other one indicates that the chiral sheet membranes provide a chiral environment for the preferential absorption of one enantiomer over the other one in racemic amino acid solution, which is attributed to the lateral arrangements of the helical fibers. This is further supported by a lack of binding activity of the nanofibers at diluted conditions (Figure S17). Interestingly, the fluorescence enhances remarkably on trapping the guests (Figure 4c), which could be attributed to the additional restricted rotation of the phenyl groups on the

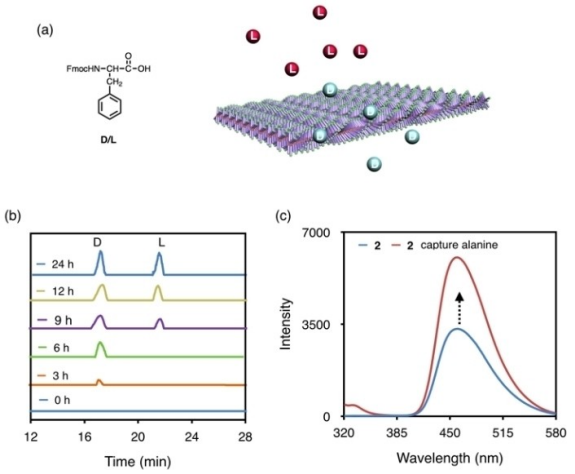

Figure 4. (a) Schematic representation of capture and chiral separation of racemic phenylalanine with **2**; (b) HPLC chromatograms of racemic phenylalanine; (c) fluorescent emission of **2** and **2** capture of hydrophobically protected phenylalanine over 6 h after adding the guest into the sheet solution.

aromatic backbone when the guest is trapped inside the chiral void space of the sheet.[27] It should be noted that the fluorescence emission remains unchanged in the case of L-enantiomer (Figure S16). This result demonstrates that the lateral arrangement of the helical fibers enables the chiral sheets to preferentially absorb one enantiomer from a racemic mixture solution with fluorescence enhancement. The fluorescence enhancement endows the chiral sheet structures with enantiomer sensing property.[28]

In summary, our results described herein demonstrate that the TPE-based amphiphiles self-assemble into stable 2D sheet structures in aqueous solution including 50 mM KF. The tetra-substituted molecule forms the nonchiral sheet structure, while the di-substituted molecule forms the chiral sheet structure. The chiral sheets arise from the lateral assembly of helical fibers, which function as selective enantiomer absorption membrane with chiral sensing. We believe that such chiral sheet structure formed from the self-assembly of AIE molecules will offer an opportunity to develop novel enantiomer separation materials with sensing characteristics.

Acknowledgements

This work was supported by the National Natural Science Foundation of China (21634005 and 21971084).

Conflict of Interest

The authors declare no conflict of interest.

Keywords: aggregation-induced emission · chiral sheets · enantiomer sorption · self-assembly · sensing

[1] T. Ryosuke, Y. Taihei, S. Kazuki, K. Kenta, *Macromolecules* **2014**, *47*, 6382–6388.
[2] J. Luo, Z. Xie, J. W. Y. Lam, L. Cheng, B. Z. Tang, H. Chen, C. Qiu, H. S. Kwok, X. Zhan, Y. Liu, D. Zhu, *Chem. Commun.* **2001**, *37*, 1740–1741.
[3] Y. Hong, J. W. Y. Lam, B. Z. Tang, *Chem. Commun.* **2009**, *45*, 4332–4353.
[4] H. Liu, J. Xu, Y. Li, Y. Li, *Acc. Chem. Res.* **2010**, *43*, 1496–1508.
[5] Y. Zhang, D. Li, Y. Li, J. Yu, *Chem. Sci.* **2014**, *5*, 2710–2716.
[6] Y. Gao, Y. Qu, T. Jiang, H. Zhang, N. He, B. Li, J. Wu, J. Hua, *J. Mater. Chem. C* **2014**, *2*, 6353–6361.
[7] X. Wang, J. Hu, G. Zhang, S. Liu, *J. Am. Chem. Soc.* **2014**, *136*, 9890–9893.
[8] B.-K. An, S.-K. Kwon, S.-D. Jung, S.Y. Park, *J. Am. Chem. Soc.* **2002**, *124*, 14410–14415.
[9] S.-J. Lim, B.-K. An, S. D. Jung, M.-A. Chung, S. Y. Park, *Angew. Chem. Int. Ed.* **2004**, *43*, 6346–6350; *Angew. Chem.* **2004**, *116*, 6506–6510.
[10] Q. Liu, Q. Xia, S. Wang, B. S. Li, B. Z. Tang, *J. Mater. Chem. C* **2018**, *6*, 4807–4816.
[11] G. Fernández, F. García, F. Aparicio, E. Matesanz, L. Sánchez, *Chem. Commun.* **2009**, *45*, 7155–7157.
[12] P. P. Kapadia, J. C. Widen, M. A. Magnus, D. C. Swenson, F. C. Pigge, *Tetrahedron Lett.* **2011**, *52*, 2519–2522.
[13] Y.-R. Zheng, Z. Zhao, M. Wang, K. Ghosh, J. B. Pollock, T. R. Cook, P. J. Stang, *J. Am. Chem. Soc.* **2010**, *132*, 16873–16882.
[14] G. Huang, G. Zhang, D. Zhang, *Chem. Commun.* **2012**, *48*, 7504–7506.
[15] F. C. Pigge, P. P. Kapadia, D. C. Swenson, *CrystEngComm* **2013**, *15*, 4386–4391.
[16] a) J. Wang, J. Mei, R. Hu, J. Z. Sun, A. Qin, B. Z. Tang, *J. Am. Chem. Soc.* **2012**, *134*, 9956–9966; b) K. Mandal, D. Jana, B. K. Ghorai, N. R. Jana, *J. Phys. Chem. C* **2016**, *120*, 5196–5206; c) M. J. Chang, K. Kim, C. Kang, M. H. Lee, *ACS Omega* **2019**, *4*, 7176–7181.
[17] a) X. Y. Shen, Y. J. Wang, E. Zhao, Z. Y. Wang, Y. Liu, P. Lu, A. Qin, Y. Ma, J. Z. Sun, B. Z. Tang, *J. Phys. Chem. C* **2013**, *117*, 7334–7347; b) Q. Zhao, S. Zhang, Y. Liu, J. Mei, S. Chen, P. Lu, A. Qin, Y. Ma, J. Z. Sun, B. Z. Tang, *J. Mater. Chem.* **2012**, *22*, 7387–7394.
[18] a) H.-T. Feng, S. Song, Y.-C. Chen, C.-H. Shen, Y.-S. Zheng, *J. Mater. Chem. C* **2014**, *2*, 2353–2359; b) S. Song, H.-F. Zheng, H.-T. Feng, Y.-S. Zheng, *Chem. Commun.* **2014**, *50*, 15212–15215.
[19] M. Liu, L. Zhang, T. Wang, *Chem. Rev.* **2015**, *115*, 7304–7397.
[20] H.-J. Kim, T. Kim, M. Lee, *Acc. Chem. Res.* **2011**, *44*, 72–82.
[21] a) Y. Hong, J. W. Y. Lam, B. Z. Tang, *Chem. Soc. Rev.* **2011**, *40*, 5361–5388; b) J. B. Zhang, B. Xu, J. L. Chen, S. Q. Ma, Y. J. Dong, L. J. Wang, B. Li, L. Ye, W. J. Tian, *Adv. Mater.* **2014**, *26*, 739–745.
[22] A. Rananaware, R. S. Bhosale, H. Patil, M. A. Kobaisi, A. Abraham, R. Shukla, S. V. Bhosale, S. V. Bhosale, *RSC Adv.* **2014**, *4*, 59078–59082.
[23] a) S. Wu, Y. Li, S. Xie, C. Ma, J. Lim, J. Zhao, D. S. Kim, M. Yang, D. K. Yoon, M. Lee, S. O. Kim, Z. Huang, *Angew. Chem. Int. Ed.* **2017**, *56*, 11511–11514; *Angew. Chem.* **2017**, *129*, 11669–11672; b) M. Shirakawa, S. Kawano, N. Fujita, K. Sada, S. Shinkai, *J. Org. Chem.* **2003**, *68*, 5037–5044.
[24] Y. Wang, Z. Huang, Y. Kim, Y. He, M. Lee, *J. Am. Chem. Soc.* **2014**, *136*, 16152–16155.
[25] a) B. Shen, Y. He, Y. Kim, Y. Wang, M. Lee, *Angew. Chem. Int. Ed.* **2016**, *55*, 2382–2386; *Angew. Chem.* **2016**, *128*, 2428–2432; b) E. Lee, J.-K. Kim, M. Lee, *Angew. Chem. Int. Ed.* **2008**, *47*, 6375–6378; *Angew. Chem.* **2008**, *120*, 6475–6478.
[26] a) J. Shen, Y. Okamoto, *Chem. Rev.* **2016**, *116*, 1094–1138; b) X. Chen, Y. He, Y. Kim, M. Lee, *J. Am. Chem. Soc.* **2016**, *138*, 5773–5776; c) X. Chen, Y. Wang, H. Wang, Y. Kim, M. Lee, *Chem. Commun.* **2017**, *53*, 10958–10916.
[27] a) B. Sun, Y. Kim, Y. Wang, H. Wang, J. Kim, X. Liu, M. Lee, *Nat. Mater.* **2018**, *17*, 599–604; b) R. Xie, L.-Y. Chu, J.-G. Deng, *Chem. Soc. Rev.* **2008**, *37*, 1243–1263.
[28] a) X. Wu, X. Han, Q. Xu, Y. Liu, C. Yuan, S. Yang, Y. Liu, J. Jiang, Y. Cui, *J. Am. Chem. Soc.* **2019**, *141*, 7081–7089; b) C. Zhang, C. Liu, X. Xue, X. Zhang, S. Huo, Y. Jiang, W.-Q. Chen, G. Zou, X.-J. Liang, *ACS Appl. Mater. Interfaces* **2014**, *6*, 757–762; c) M. Kawai, A. Hoshi, R. Nishiyabu, Y. Kubo, *Chem. Commun.* **2017**, *53*, 10144–10147.

Manuscript received: February 25, 2020
Revised manuscript received: March 24, 2020
Accepted manuscript online: March 24, 2020